2016

Numerical Simulation on Heat Transfer Performance of Silicon Carbide/ Nitrate Composite for Solar Power Generation

Ruixin Zhou
School of Energy and Power Engineering, Xi'an Jiaotong University, China, zhouruixin@stu.xjtu.edu.cn

Xiaole Chen
School of Energy and Power Engineering, Xi'an Jiaotong University, China, chenxiaole@stu.xjtu.edu.cn

Yang Lu
School of Energy and Power Engineering, Xi'an Jiaotong University, China, ly0317@stu.xjtu.edu.cn

Bei Guo
School of Energy and Power Engineering, Xi'an Jiaotong University, China, guobei@xjtu.edu.cn

Numerical Simulation on Heat Transfer Performance of Silicon Carbide /Nitrate Composite for Solar Power Generation

Ruixin ZHOU, Xiaole CHEN, Yang LU, Bei GUO*

School of Energy and Power Engineering, Xi'an Jiaotong University, China

*Corresponding Author: Bei Guo, School of Energy and Power Engineering, Xi'an Jiaotong University, No.28 Xianning West Road, Xi'an, Shaanxi 710049, PR China. Email: guobei@mail.xjtu.edu.cn

Abstract

KNO_3 was used as the phase change material (PCM), but its thermal conductivity is too low to transfer heat between the PCM and conduction oil efficiently. In this thesis, on the basis of the previous studies (Yong Li, 2015), the solar power generation efficiency is enhanced with high temperature interval (280℃—400℃), and the new composite which are composed by the SiC honeycomb (SCH) frame and infiltrated KNO_3 is simulated by using Fluent software. The 2-D model is set up according to the cylindrical structure of the thermal energy storage units (TESU) and the 3-D models are set up with triangular arrangement of the pipes for the module thermal energy storage tank (MTEST).The results show that the new composite of the KNO_3 +30%SCH suit for the requirement of the charging time and capacity in the design of the TESU; The comparable simulation for the long and short pipe models supplies the evidences that the long pipe simulation can be substituted by the short pipe simulation, which reduces the 3-D simulation time enormously; The comparable simulation of the radial dimensions supplies some theory foundations for the design of the MTEST . These simulation results have important guidance on the design of the thermal energy storage unit and the module thermal energy storage tank.

Keywords: phase change material, thermal energy storage unit, SiC honeycomb, numerical simulation, solar power generation

1. Introduction

The 98% of energy on the earth is brought from the sun shine. However the energy density of the dispersive sun shine is very small, and thus it is difficult to re-collect and utilize it as a heat source, not to mention, to utilize it for generating electricity. The heat storage technology which makes it possible to use solar energy continuously can be used to collect discontinuous and unstable solar energy. Latent heat thermal energy storage (LHTES) using phase change material (PCM) has attracted great interests due to its large energy storage capacity during the phase change process (Agyenim *et al.*,2010; Ming *et al.*,2012). Yong Li (2015) chosen the $KNO_3/NaNO_3$ (50/50mol%) mixed with SiC ceramic honeycomb (SCH) as PCM and carried out the charging and discharging experiment to test the cylindrical thermal energy storage units (TESU) with different mass fractions of SCH. Numerical simulation for the charging and discharging process of the TESU was also studied and compared with its experiment. Cabeza (2006) found natural expanded graphite is a better choice owing to its better absorbent and high porosity by applying the composite materials of PCM and graphite to the heat storage container with thermal stratification.

In this thesis, in order to enhance the solar power generation efficiency and on the basis of the previous studies (Yong Li, 2015), the temperature interval is increased as 280℃ to 400℃. The new material is chosen as the synthetic oil DOWTHERM A and the molten salt KNO_3 which are different from the eutectic salt KNO3/NaNO3(50/50mol%) and mineral oil. The charging and discharging process models with new materials are reset. The temperature of the monitoryy vertexes and the heat flux of the facets are simulated. Firstly the charging time and charging capacity is acquired which can be used to design the subsequent experiments on the TESU. Then the comparisons between the long and short models are carried out. Finally the influence of the charging and discharging process by the different oil pipe diameters and intervals are analyzed, which would lay a foundation of the design on the module thermal energy storage tank (MTEST).

2. The phase change materials and the conduction oil

2.1 The phase change materials

The properties of the molten salt KNO_3 and eutectic salt $KNO_3/NaNO_3$(50/50mol%) are shown in Table 1.

Table 1: The properties comparison between the pure PCM

Properties(Units)	KNO_3		$KNO_3/NaNO_3$	
	Temperature	Property	Temperature	Property
Density(Kg/m^3)	570K	1899.47	495K	1920
	600K	1877.6		
	630K	1856	900K	1745
	670K	1827		
Specific heat capacity(J/Kg.K)	570K	1350	1500	
	590K	1400		
	600K	1430		
Viscosity(Kg/m.s)	620K	0.002766	0.0027	
	640K	0.002479		
	660K	0.002226		
Thermal conductivity(W/m.k)	0.5		0.5	
Pure solvent melting heat(J/Kg)	106340		99143	
Solidus Temperature(K)	607		493	

As we can see in table 1, except that KNO_3 has higher solidus temperature than the eutectic salt, there are little difference on their other properties. Because of the low thermal conductivity of the pure molten salt, the high-thermal conductive materials are added to the pure phase change material to increase its thermal conductivity.. In recent years, because of the high conductivity, low density and high stability, the graphite is widely studied and used as the thermal conductor to enhance heat transfer (Meshling, 2008; Zhang P,2010; Bauer T, 2006; Lopez J, 2010; Pincemin S, 2008). The previous studies (Yong Li, 2015) found that 30% SCH is the best choice considering the balance between the heat capacity and heat charge rate. The properties comparison between the pure PCM mixed by 30% SCH is shown in Table 2.

Table 2: The properties comparison between the pure PCM mixed by 30%SCH

Properties(Units)	KNO_3+30%SCH		$KNO_3/NaNO_3$+30%SCH	
	Temperature	Property	Temperature	Property
Density(Kg/m^3)	570K	1884.629	495K	1920
	600K	1869.32		
	630K	1854.2	900K	1745
	670K	1833.9		

Specific heat capacity (J/Kg.K)	1250	1350
Thermal conductivity(W/m.K)	3	3
Viscosity(Kg/m.s)	0.0024	0.0027
Pure solvent melting heat(J/Kg)	74438	69400
Solidus Temperature(K)	607	493

2.2 The conduction oil

The mineral oil will decompose when the temperature reach to 400℃ and its original temperature interval is 180℃ to 300℃ in the previous study (Yong Li, 2014). But the synthetic oil DOWTHERM A can suit higher temperature interval 280℃ to 400℃. As is shown in Table 3, there are little differences between the two types of the conduction oil except the viscosity.

Table 3: The comparison between the conduction oil

Properties(Units)	**DOWTHERM A**		**Mineral Oil**
	Temperature	**Property**	
Density（Kg/m^3）	528K	854	847
	578K	801.3	
	628K	742.3	
	678K	672.5	
Specific heat capacity（J/Kg.K）	528K	2231	2420
	578K	2373	
	628K	2527	
	678K	2725	
Thermal conductivity(W/m.K)	528K	0.1011	0.104
	578K	0.0931	
	628K	0.0851	
	678K	0.0771	
Viscosity (Kg/m.s)	528K	0.00027	0.003
	578K	0.0002	
	628K	0.00016	
	678K	0.00012	
Dynamic vicousity (m^2/s)	528K	3.16159*10-7	3.54191*10-7
	578K	2.49594*10-7	
	628K	2.15546*10-7	
	678K	1.78439*10-7	

3. Numerical simulation model

3.1 The 2-D model

In this thesis, the TESU is the axisymmetric facility and shown in figure 1, so an half of the cross-section is modeled on the basis of the symmetry characteristic. The 2-D sketch of the 0.5m TESU is shown in figure 2 and the meshes are generated in the insulator, PCM and oil areas.

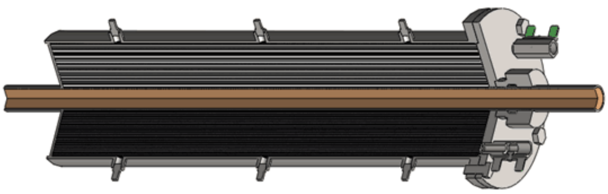

Figure 1: The cross-section of the TESU

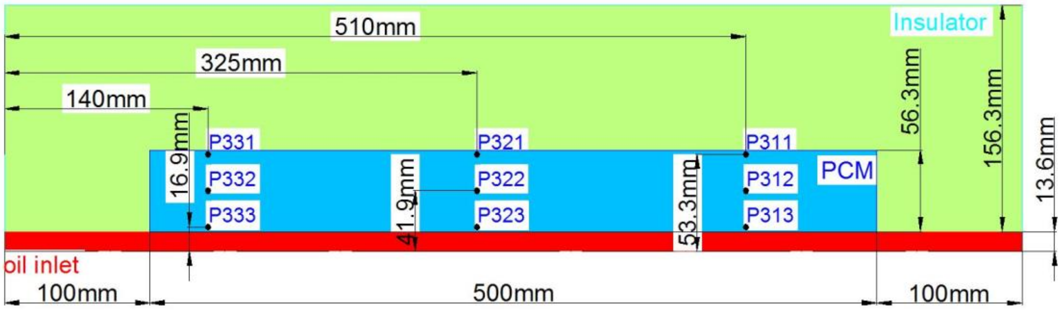

Figure 2: The 2-D sketch of 0.5m thermal energy storage unit

The model is built up according to the symmetry of the cylindrical structure. As is shown in Figure 2, the diameter of the oil pipe is 13.6mm, the thickness of the PCM is 49.1mm and the axial length of the PCM is 500mm. In order to compare with the subsequent experiments, the insulator zone is also designed in the 2-D model to simulate the influence of the insulator in experiment. The density of the insulator is 160Kg/m^3, and its specific heat capacity is 1128J/Kg.K.

The Gambit software is used to model and generate mesh. The numerical calculation is carried out by the fluent software. The inlet boundary condition is “velocity inlet” and the velocity rate is 0.4m/s. The hydraulic diameter is 23.2mm and the turbulent intensity is 6%. The temperature of the inlet oil is 673K while charging process and 563k while discharging process. The adiabatic condition is set on the insulator wall. 9 monitory points in the PCM and the monitory facet at the oil pipe outlet are set to monitor their temperature variation. The monitory facet at the oil pipe wall is also set to monitor the heat flux into the PCM and insulator.

3.2 The 3-D model

The 2-D model only simulates the heat transfer of single pipe. But the actual heat transfer in the module thermal energy tank (MTEST) is influenced by multi-pipes, and the charging and discharging simulation in the MTEST is different from the 2-D model. In order to guarantee the uniform temperature distribution in the MTEST, the triangular arrangement of the pipes is applied.

To sum up, the 3-D model with triangular arrangement of the pipes is set up and shown in the figure 3. The radial dimension sketch of the 3 pipes is shown in the figure 4. Considering the multi-pipes arrangement in the MTEST, The shell of the PCM is set as adiabatic condition. The insulator in the 2-D model is to simulate its influence of the heat transfer and to analysis the experiment and simulation of the TESU.

Figure 3: The pipe arrangement method

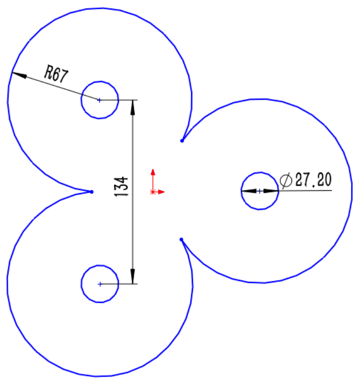

Figure 4: The radial dimension sketch of the three pipes

The requirements in the design of the MTEST are 10m pipes. But the simulation of the 10m model is very slow and the 10m pipes are difficult to realize in experiment. The relationships between the long and short models are analyzed aiming to substitute the short model for the long model. The modeling and simulation are carried out on the three pipes of 0.5m, 2m and 10m and three type models can show the relationships in detail. All of them are arranged in triangle shape and all their boundaries of the simulation zone are set as adiabatic conditions. Other boundary conditions and the monitors for these three models are all set as the same values.

The comparative simulation shows that the charging time and storage capacity of the short models are in proportion with the long models'. In order to shorten the calculation time and find out the relationships between the heat storage time and the radial dimension of the models, the 3-D pipes of 0.5m is chosen to simulate. Five models are built up by altering the pipe diameter and interval, and then the relationship between the heat storage time and the radial dimension can be deduced. The detail radial dimensions of the MTEST are shown in Table 4.

Table 4: The radial dimensions of the MTEST

Number	Pipe diameter(mm)	Pipe interval(mm)
1	27.2	67
2	27.2	85
3	27.2	100
4	30	67
5	32	67

In theory, the point (0, 0, 500mm), which is the farthest point from the oil pipes in the PCM and at the outlet side of the PCM, is the slowest point of the temperature variation in the PCM area. The temperature variation at the point (0, 0, 500mm) in the model is deemed as the temperature variation of the whole MTEST. The heat flux through the oil pipes is deemed as the charging and discharging capacity because the boundary of the simulation zone is set as adiabatic condition.

4. Simulation results and analysis

4.1 The 2-D simulation results and analysis

According to the 2-D model sketch and the corresponding setting method shown in Figure 2, the time and capacity of the charging and discharging process are simulated. In order to observe the law of the temperature distribution, the second hour is set as the deadline of heat storage and releasing process, Figure 5 shows the temperature distribution of the material in the process of heat storage at the moment and Figure 6 shows the temperature distribution of that in the process of heat release at the moment.

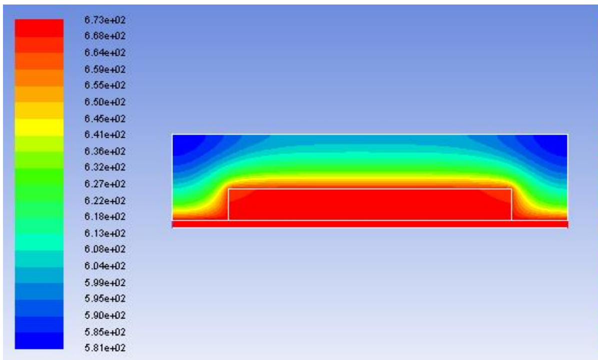

Figure 5: The temperature contour of the

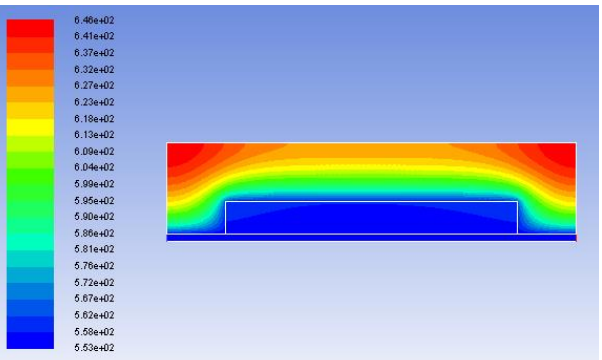

Figure 6: The temperature contour of the

heat storage process heat release process

From the Figure 5 and 6, the temperature distribution of the storage material and insulator material at the second hour is shown in detail. Since the boundary of the insulator materials was set as adiabatic conditions, the temperature of the outermost insulator materials changes very slowly.

Figures 7 and 8, respectively, summarized the temperature variation of the three monitory points P311, P312 and P313 which are at the outlet side of the PCM and have slower temperature variation in the charging and discharging process. Figure 9 demonstrates the heat flux variation during charging and discharging process.

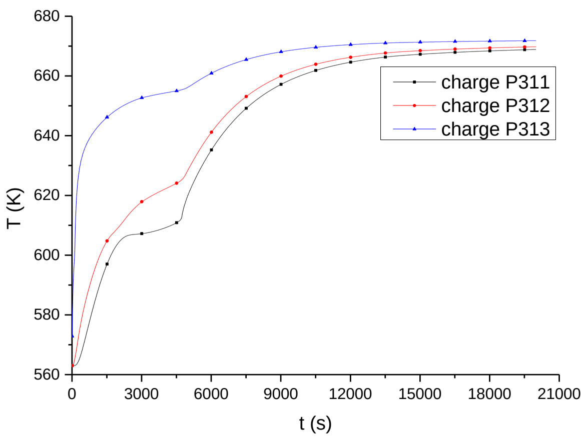

Figure 7: Temperature variation of charging process at radial direction

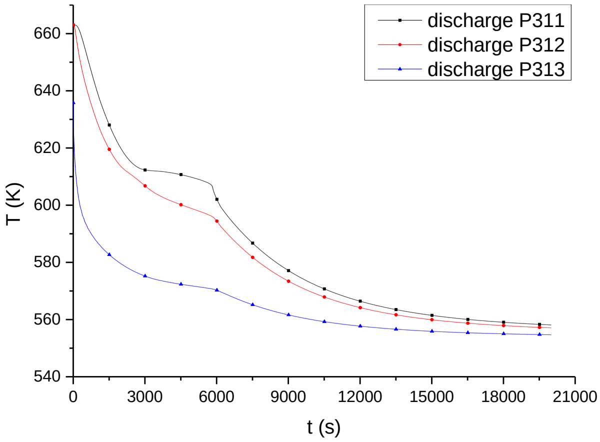

Figure 8: Temperature variation of discharging process at radial direction

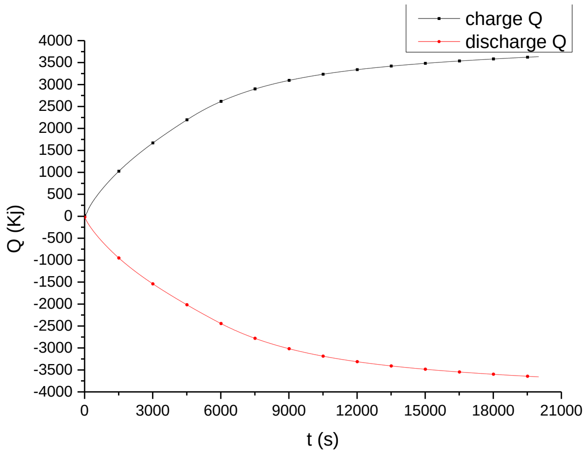

Figure 9: The heat flux variation of the charge and discharge process

The zones where the temperature curves appear the small variation steps in Figure 7 and 8 are called phase transition zones. If the deadline of temperature of the charging process is 663K and the temperature of discharging process is 563K, the deadline of the charging process is about 3.22 hours and the deadline of the discharging process is about 3.67 hours according to the simulation results. Because the insulator material was considered in the simulation for the subsequent experiment validation, the time of charging and discharging process must longer than that there are no insulator in the model.

4.2 The 3-d simulation results and analysis

4.2.1 The comparison between the long and short 3-D pipes

In theory, the lowest point of charging and discharging process at the radial direction should be at the center of the three pipes and the lowest facet of charging and discharging process at the axial direction should be at the outlet side of the PCM. After transient simulation of the 3-D tubes of 10m, the temperature contour of the third hour is showed as Figure 10. The simulation results shown in Figure 10 are in accordance with the temperature distribution in theoretical analysis. In order to find out the disciplinarian of the rate of long and short tubes in the charging and discharging process, the research set the same boundary conditions for the 3-D pipes of 0.5m, 2m and 10m. Figure 11 contrasts the temperature variations of 0.5m tubes, 2m tubes and 10m tubes at the same point(0,0,500mm). Figure 12 contrasts the temperature variation at the center of the outlet side facet of the PCM.

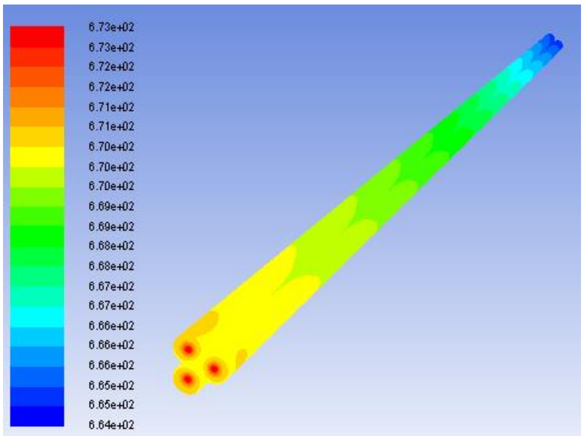

Figure 10: The temperature contour of the third hour of the 10m three tubes

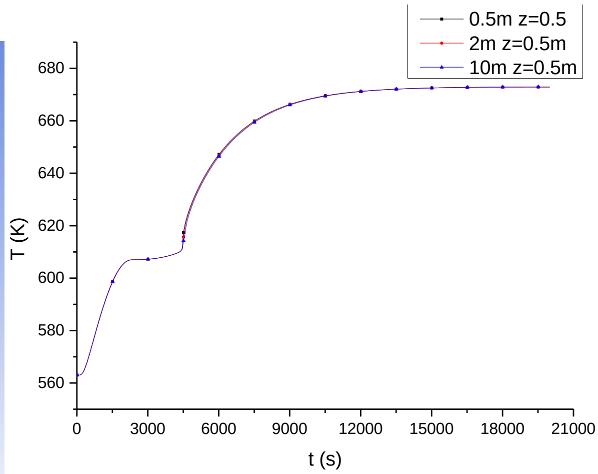

Figure 11: The temperature variations at the point(0,0,500mm)

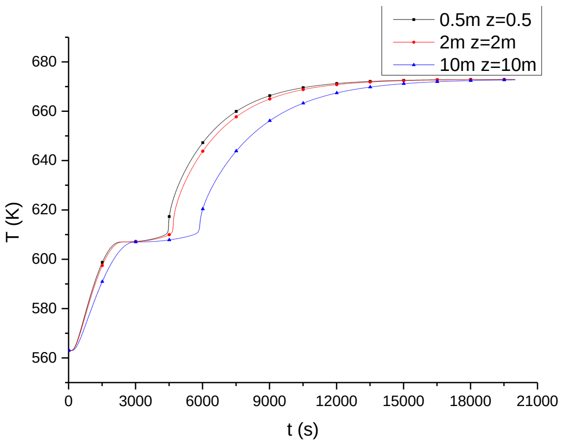

Figure 12: The temperature variations at the outlet side facet centers

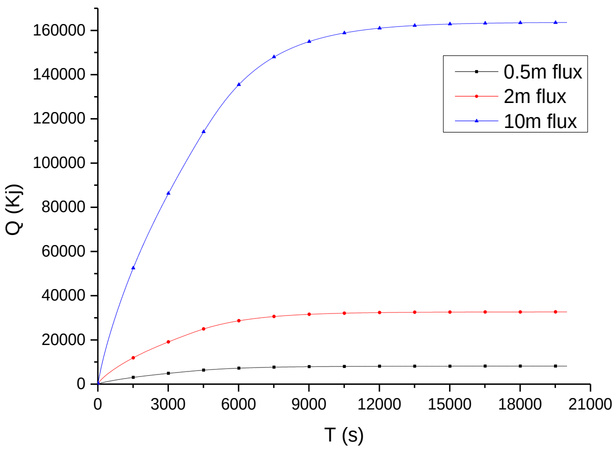

Figure 13: The heat storage capacity of the three dimension kinds

The three dimension sizes has similar temperature variation at the same point shown in Figure11. According to Figure 12, the PCM heat storage rates of long tubes are lower than those of short tubes at the oil outlet. Figure 13 contrasts the heat storage capacity of the three dimension sizes. Because the outlet side facet center of PCM is the slowest point while charging, their temperatures of the three dimension sizes are set as symbols of heat storage variation. The charging time and capacity of the three dimension kinds are shown in Table 5.

Table 5: The heat charging time and capacity of the three dimension kinds

Axial dimension	Heat charging time （hour）	Heat charging capacity （Kj）	Heat charging capacity per unit length (Kj/m)
0.5m	2.31	7809.92	15619.84
2m	2.43	31434.06	15717.03
10m	2.98	159240.63	15924.063

Comprehensively speaking, the heat charging capacity per unit length of the three models, which are shown in Table 5, are similar. The deviations of the 0.5m and 2m model with respect to the 10m model are just 1.9% and 1.3% separately. It can be known that the heat storage rate of the 10m tubes is comparatively lower, but the trend of the temperature variation is consistent among the long and short pipes. The three dimension kind's models with the same radial dimensions (pipe diameter is 27.2mm and the pipes interval is 67mm) are simulated, and the heat charging time and capacity are shown in table 5. When the radial dimension is changed and its 0.5m model is calculated, the 10m model can be deduced in proportion with the charging time shown in table 5. In order to study the relationships between the heat storage rate and the radial dimensions, the 3-D pipes model of 0.5m is chosen to calculate in the following works.

4.2.2 The 3-D simulation of the short pipes and the design of the pipes arrangement

According to the radial dimensions shown in Table 4, the models of 0.5m are built up and calculated. Through monitoring the center of the outlet side facet of the PCM, the temperature variations of different radial dimensions at the same point position are shown following. The heat flux of the charging and discharging process varied by time is also monitored on the oil pipe wall, and their variations are also shown below.

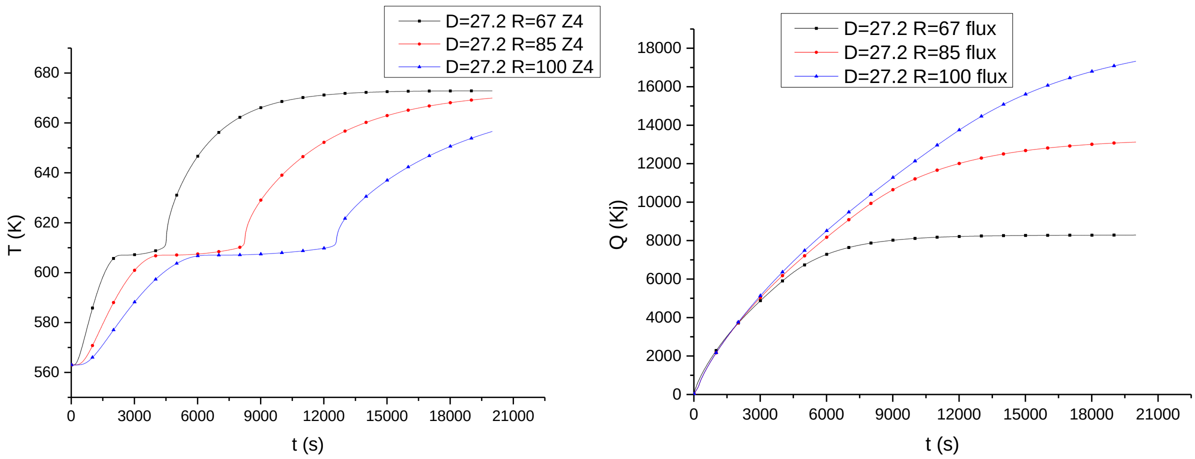

Figure 14: The temperature and heat flux variations of the same pipe diameters but different intervals while charging

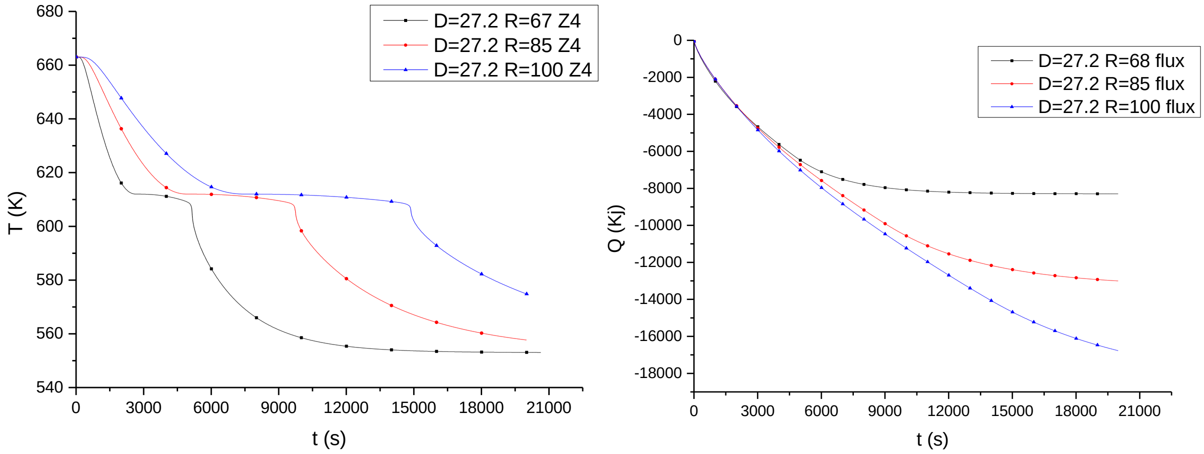

Figure 15: The temperature and heat flux variations of the same diameters but different intervals while discharging

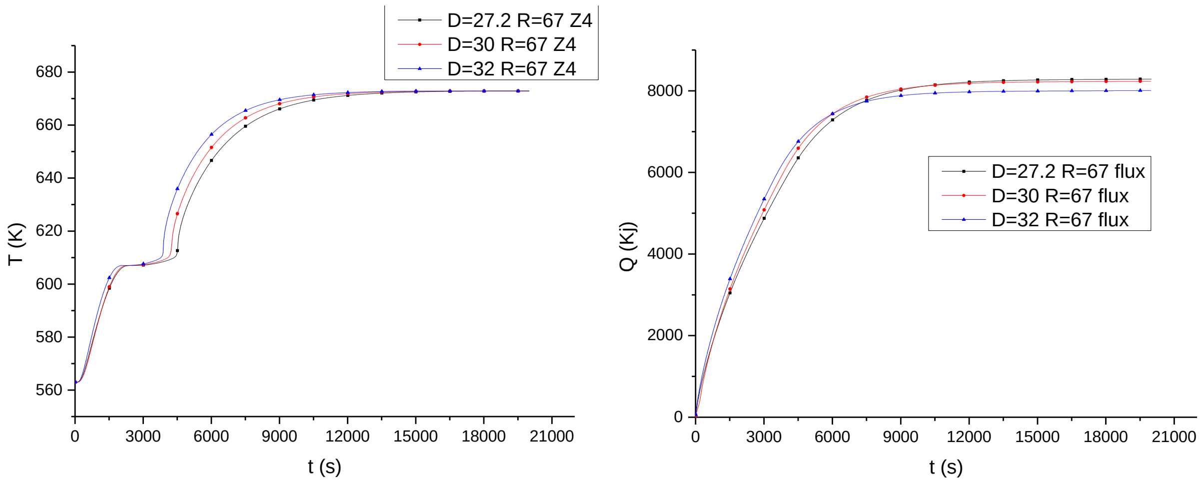

Figure 16: The temperature and heat flux variations of the same pipe intervals but different diameters while charging

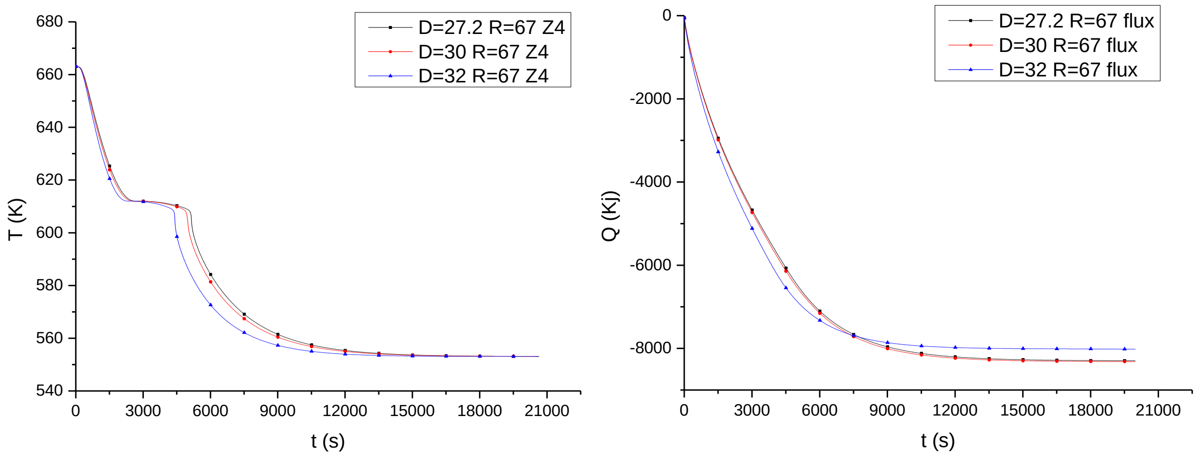

Figure 17: The temperature and heat flux variations of the same pipe intervals but different diameters while discharging

Based on the above results comparison, the time of charging and discharging process is decreasing with the increase of the pipe diameters and the time of charging and discharging is increasing with the increase of the intervals. That is to say, the charging and discharging rates have some mathematical relations with the pipe diameters and intervals. In actual designing, the pipe diameters and intervals should be designed according to the actual working conditions to control the cost and maximize efficiency.

5. Conclusion

Because the charging and discharging process with higher temperature interval can produce higher quality steam to generate electricity, the efficiency of solar heat storage and electricity generation is increasingly improved by enhancing the temperature range which is realized by changing the material and oil. Based on the verified simulation method proposed by Liyong(2015) which have proved that only considering thermal conductivity can macthes well with the experiments, the research has achieved the following results: Firstly, through the 2-D simulation, the heat storage time and heat storage flux with insulator are acquired which can be used to plan and design the subsequent experiments on the TESU. Secondly, through the comparisons between the long and short models, the relationships between the long and short models are more clearly. The method of simulating the MTEST by the model of 0.5m is proved to be feasible and convenient. Finally, the influence of the charging and discharging process by the different oil pipe diameters and intervals were also analyzed, which would lay a foundation of the design on the module thermal energy storage tank (MTEST). The results mentioned above have guiding significance in designing heat storage appliances with higher efficiency.

References

Agyenim, F., et al., A review of materials, heat transfer and phase change problem formulation for latent heat thermal energy storage systems (LHTESS). *Renewable & Sustainable Energy Reviews*, 2010. 14(2): p. 615-628.

Ming, L., W. Saman, and F. Bruno, Review on storage materials and thermal performance enhancement techniques for high temperature phase change thermal storage systems. *Renewable and Sustainable Energy Reviews*, 2012. 16(4): p. 2118-32.

Li Y, Guo B, Huang G, et al. Characterization and thermal performance of nitrate mixture/SiC ceramic honeycomb composite phase change materials for thermal energy storage[J]. *Applied Thermal Engineering*, 2015, 81:193-197.

Cabeza LF, Ibanez M, Sole C, et a1.Experimentation with water tank including a PCM module[J]. *Solar Energy Mater Sol Cells*,2006,90:1273-1782

Mehling H, Cabeza LF. Heat and cold storage with PCM – an up to date introduction into basics and applications. Berlin, Germany: Springer; 2008.

Zhang P, Song L, Lu H, Wang J, Hu Y. The influence of expanded graphite on thermal properties for paraffin/high density polyethylene/chlorinated paraffin/antimony trioxide as a flame retardant phase change material[J]. *Energy Conversion and Management*.2010;51:2733 – 7.

Bauer T, Tamme R, Christ M, O˝ ttinger O. PCM-graphite composites for high temperature thermal energy storage[C]. *In: Ecostock’ 2006—10th international conference on thermal energy storage*. 2006.

Lopez J, Caceres G, Palomo Del Barrio E, Jomaa W. Confined melting in deformable porous media: a first attempt to explain the graphite/salt compositesbehaviour[J]. *International Journal of Heat and Mass Transfer* 2010;53:1195 – 207.

Pincemin S, Olives R, Py X, Christ M. Highly conductive composites made of phase change materials and graphite for thermal storage[J]. *Solar Energy Materialsand Solar Cells* 2008;92:603 – 13.